Use of Physiologically Based Biokinetic (PBBK) Modeling to Study Estragole Bioactivation and Detoxification in Humans as Compared with Male Rats

Ans Punt,*,†,1 Alicia Paini,*,† Marelle G. Boersma,* Andreas P. Freidig,‡ Thierry Delatour,† Gabriele Scholz,† Benoît Schilter,†
Peter J. van Bladeren,*,† and Ivonne M. C. M. Rietjens*

*Division of Toxicology, Wageningen University, 6703 HE Wageningen, The Netherlands; †Nestlé Research Center, Lausanne, Switzerland; and ‡Amsterdam
Molecular Therapeutics, 1100 DA Amsterdam, The Netherlands

The extent of bioactivation of the herbal constituent estragole to its ultimate carcinogenic metabolite 1′-sulfooxyestragole depends on the relative levels of bioactivation and detoxification pathways. The present study investigated the kinetics of the metabolic reactions of both estragole and its proximate carcinogenic metabolite 1′-hydroxyestragole in humans in incubations with relevant tissue fractions. Based on the kinetic data obtained a physiologically based biokinetic (PBBK) model for estragole in human was defined to predict the relative extent of bioactivation and detoxification at different dose levels of estragole. The outcomes of the model were subsequently compared with those previously predicted by a PBBK model for estragole in male rat to evaluate the occurrence of species differences in metabolic activation. The results obtained reveal that formation of 1′-oxoestragole, which represents a minor metabolic route for 1′-hydroxyestragole in rat, is the main detoxification pathway of 1′-hydroxyestragole in humans. Due to a high level of this 1′-hydroxyestragole oxidation pathway in human liver, the predicted species differences in formation of 1′-sulfooxyestragole remain relatively low, with the predicted formation of 1′-sulfooxyestragole being twofold higher in human compared with male rat, even though the formation of its precursor 1′-hydroxyestragole was predicted to be fourfold higher in human. Overall, it is concluded that in spite of significant differences in the relative extent of different metabolic pathways between human and male rat there is a minor influence of species differences on the ultimate overall bioactivation of estragole to 1′-sulfooxyestragole.

Key Words: estragole; PBBK; human; metabolism; *in vitro*; species differences.

Estragole is an alkenylbenzene that occurs naturally in certain herbs such as tarragon, basil, and fennel, and in essential oils of these herbs used as flavoring agents (Smith *et al.*, 2002). At high dose levels this compound is found to be hepatocarcinogenic in different rodents (Drinkwater *et al.*, 1976; Miller *et al.*, 1983; Wiseman *et al.*, 1987). Uncertainties about the shape of the dose-response curve at dose levels relevant for dietary human intake and about species differences in metabolism and metabolic activation make it difficult to extrapolate the cancer risk from high dose animal experiments to the low dose human situation. In an evaluation performed by the expert panel of the Flavor and Extract Manufacturers Association (FEMA) it was concluded that exposure to estragole from herbs, essential oils, and flavor substances does not pose a significant cancer risk to humans (Smith *et al.*, 2002). In this conclusion, experimental data that suggested a nonlinear relationship between dose and profiles of metabolism and metabolic activation were taken into account. The FEMA expert panel estimated the average daily intake of estragole to be less than 0.01 mg/kg bw/day, which was determined based on production volume data for flavor use (Smith *et al.*, 2002). The Scientific Committee on Food (SCF) of the European Union concluded in their evaluation of estragole, that estragole is genotoxic and carcinogenic, and restrictions in use levels were indicated (SCF, 2001). The SCF estimated the average daily intake of estragole from all food sources to be 4.3 mg/day, corresponding to ~0.07 mg/kg bw/day for a 60 kg person (SCF, 2001). This estimation is based on theoretical maximum use levels of estragole in various food categories and consumption data for these food categories.

Rodent carcinogenicity of estragole has been linked to its metabolic conversion to a genotoxic metabolite (Drinkwater *et al.*, 1976; Miller *et al.*, 1983; Wiseman *et al.*, 1987). Bioactivation of estragole starts with the conversion of estragole into the proximate carcinogenic metabolite 1′-hydroxyestragole (Fig. 1), which is mainly catalyzed by cytochrome P450 1A2 and P450 2A6 (Jeurissen *et al.*, 2007). Other phase I metabolic pathways represented in Figure 1 include *O*-demethylation, epoxidation, and 3′-hydroxylation of estragole, leading to the formation of, respectively,

1 To whom correspondence should be addressed at Division of Toxicology, Wageningen University, Tuinlaan 5, 6703 HE Wageningen, The Netherlands. Fax: +31-317-484931. E-mail: ivonne.rietjens@wur.nl.
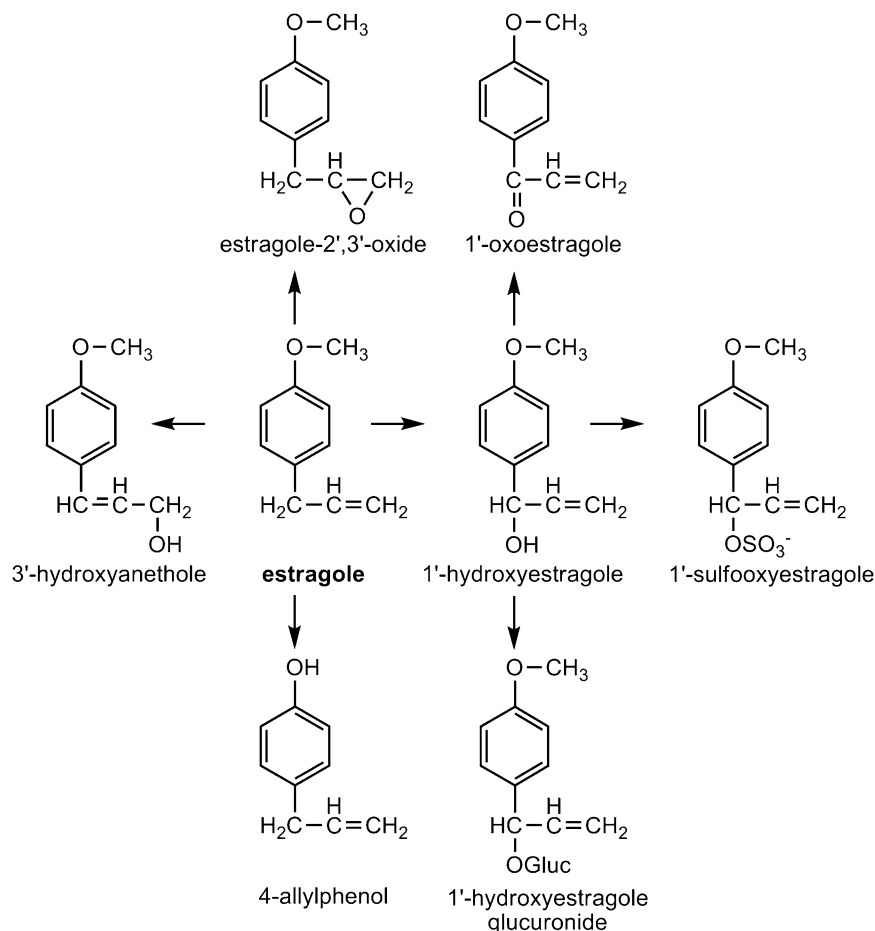
FIG. 1. Metabolism of estragole.

4-allylphenol, estragole-2′,3′-oxide, and 3′-hydroxyanethole. These metabolic pathways result in detoxification of estragole (Anthony *et al.*, 1987; Guenthner and Luo, 2001; Luo *et al.*, 1992; Phillips *et al.*, 1981; Sangster *et al.*, 1987; Solheim and Scheline, 1973). Sulfonation of 1′-hydroxyestragole leads to the formation of the ultimate carcinogenic metabolite, which is unstable and degrades in aqueous environment to a reactive carbocation that is capable of forming DNA adducts (Phillips *et al.*, 1981, 1984; Randerath *et al.*, 1984; Wiseman *et al.*, 1985). Conjugation of 1′-hydroxyestragole with glucuronic acid results in detoxification of 1′-hydroxyestragole, because it results in formation of a stable metabolite that has been detected in the urine of both humans and rats exposed to estragole (Anthony *et al.*, 1987; Sangster *et al.*, 1987). In addition to glucuronidation and sulfonation, oxidation of 1′-hydroxyestragole to 1′-oxoestragole has been reported as a possible metabolic route of 1′-hydroxyestragole (Solheim and Scheline, 1973). The 1′-oxoestragole metabolite of 1′-hydroxyestragole is a reactive metabolite that has been shown to be able to form adducts with 2′-deoxyguanosine in a direct reaction with this nucleoside (Phillips *et al.*, 1981). In spite of

this, 1′-oxoestragole was not carcinogenic *in vivo* in mice (Wiseman *et al.*, 1987). This has been ascribed to extensive detoxification of 1′-oxoestragole via conjugation with gluta-thione or endogenous amines (Fennell *et al.*, 1984; Wiseman *et al.*, 1987; Wislocki *et al.*, 1977). To date, formation of 1′-oxoestragole has been considered to be of minor importance, because only relatively small amounts of derivatives of this metabolite have been detected in the urine of rats exposed orally to [methoxy-^{14}C]-labeled estragole (Solheim and Scheline, 1973).

Dose-dependent effects in metabolism of estragole have been revealed in both rats and mice exposed to different oral doses of estragole. In these species the relative extent of *O*-demethylation decreased with increasing doses accompanied by a relative increase in excretion of 1′-hydroxyestragole glucuronide in the urine (Anthony *et al.*, 1987; Zangouras *et al.*, 1981). Based on a previously constructed physiologically based biokinetic (PBBK) model for estragole in male rat (Punt *et al.*, 2008) it was demonstrated that these dose-dependent effects could be explained by a shift in metabolism of estragole. At low oral doses, *O*-demethylation is the major metabolic

pathway, occurring mainly in the lung and kidney due to formation of this metabolite with high affinity in these organs. Saturation of this metabolic pathway in the lung and kidney at increasing oral dose levels, leads to a relative increase in formation of 1′-hydroxyestragole in the liver and a concomitant increase in formation of 1′-hydroxyestragole glucuronide and the ultimate carcinogenic metabolite, 1′-sulfooxyestragole. Such dose-dependent effects can have consequences for the extrapolation of the cancer risk from high dose animal experiments to humans at relevant dietary intake levels.

In addition to dose-dependent effects, species differences in metabolism and metabolic activation can also occur. We have, for instance, previously demonstrated that male rats are more efficient in sulfonation of 1′-hydroxyestragole than humans (Punt *et al.*, 2007). To determine the overall differences between humans and male rats in bioactivation of estragole, it is of importance to compare the relative extent of different metabolic pathways between these species. The present study investigated the kinetics of possible metabolic reactions of estragole and 1′-hydroxyestragole in humans in incubations with relevant human tissue fractions. The kinetic data obtained were used to build a PBBK model for estragole metabolism in human to predict the relative extent of bioactivation and detoxification of estragole at dose levels relevant for dietary human intake. An evaluation of the model defined was performed by comparing the predicted formation of 4-allylphenol and 1′-hydroxyestragole glucuronide to literature reported levels of these metabolites in humans exposed to estragole (Sangster *et al.*, 1987). The outcomes of the model were subsequently compared with those of the previously defined PBBK model for estragole in male rat to evaluate the occurrence of species differences in metabolic activation and detoxification of estragole.

MATERIALS AND METHODS

Chemicals and biological materials. Pooled, mixed gender human lung, kidney, and small intestine microsomes were purchased from BioPredic International (Rennes, France). Pooled, mixed gender human liver S9 and microsomes were purchased from BD Gentest (Woburn, MA). Hydrochloric acid (37%) was purchased from Merck (Darmstadt, Germany). β-Glucuronidase, nicotinamide adenine dinucleotide phosphate (reduced) (NADPH), and NAD$^+$ were obtained from Roche Diagnostics (Mannheim, Germany). Tris(hydroxymethyl)aminomethane was obtained from Gibco BRL Life Technologies (Paisley, UK). Estragole (4-allylanisol), acetonitrile (chromatography grade), methanol, dimethylsulfoxide (DMSO), ascorbic acid, alamethicin, glutathione (GSH), bovine serum albumin (BSA), uridine 5′-diphosphoglucuronic acid (UDPGA), and a GSH assay kit were purchased from Sigma-Aldrich (Steinheim, Germany). 1′-Hydroxyestragole, 4-allylphenol, estragole-2′,3′-oxide, and 3′-hydroxyanethole were synthesized as described previously (Punt *et al.*, 2008). *Caution: 1′-hydroxyestragole, 3′-hydroxyanethole, estragole-2′,3′-oxide, 1′-oxoestragole are genotoxic and should be handled accordingly.*

Phase I metabolism. Mixed gender human liver, lung, kidney, and small intestine microsomal preparations were incubated with estragole in the presence of NADPH, to identify the organs involved in the phase I metabolism of estragole. The incubation mixtures had a final volume of 100 μl, containing (final concentrations) 3mM NADPH, 1mM ascorbic acid and 1 mg/ml microsomal protein in 0.2M Tris-HCl (pH 7.4). After preincubating at 37°C for 1 min, the reactions were started by adding the substrate estragole. Initial incubations with the different microsomal fractions were performed at a substrate concentration of 100μM (final concentration) at several incubation times. The reactions were terminated by addition of 25 μl cold acetonitrile. Additional incubations to determine the kinetic constants for the formation of phase I metabolites of estragole were performed only with human liver microsomes, because these were the microsomal samples tested that resulted in metabolic conversion of estragole (see Results section). These incubations were carried out for 10 min at a substrate concentration that ranged from 10 to 400μM estragole. Under these conditions the formation of the different estragole metabolites was linear with time and microsomal protein concentration. All samples were centrifuged for 5 min at 16,000 × g and 50 μl of the supernatant of each sample was analyzed by high-performance liquid chromatography (HPLC)-UV as described previously (Punt *et al.*, 2008). In the blank incubations performed without NADPH low amounts of 3′-hydroxyanethole were formed, corresponding to approximately 0.6% of the applied concentration of estragole. For this reason the formation of 3′-hydroxyanethole was corrected for the amount of 3′-hydroxyanethole formed in the blank incubations. 3′-Hydroxyanethole was quantified by comparison of the peak areas of the metabolite in the chromatograms obtained at a wavelength of 206 nm to the calibration curve of the synthesized metabolite. Formation of 4-allylphenol and 1′-hydroxyestragole were quantified by comparison of the peak areas of the different metabolites in the chromatograms obtained at a wavelength of 225 nm to the calibration curve of the corresponding synthesized metabolites. Quantification of estragole-2′,3′-diol, which reflects formation of estragole-2′,3′-oxide (see Results section), was achieved by comparison of the peak area of estragole-2′,3′-diol in the chromatograms obtained at a wavelength of 225 nm to the calibration curve of estragole-2′,3′-oxide, because estragole-2′,3′-diol has a similar molar extinction coefficient as estragole-2′,3′-oxide (Punt *et al.*, 2008).

Glucuronidation of 1′-hydroxyestragole. Mixed gender human liver microsomal preparations were incubated with 1′-hydroxyestragole in the presence of UDPGA. The incubation mixtures had a final volume of 200 μl, containing (final concentrations) 10mM UDPGA, and 1 mg/ml microsomal protein in 0.2M Tris-HCl (pH 7.4) containing 10mM MgCl$_2$. The incubation mixtures were pre-treated on ice with 0.025 mg/ml of the poreforming peptide alamethicin from a 200 times concentrated stock solution in methanol for 15 min to overcome enzyme latency and obtain maximal glucuronidation activity (Fisher *et al.*, 2000; Lin and Wong, 2002). The reactions were started by the addition of the substrate 1′-hydroxyestragole from a 200 times concentrated stock solution in DMSO, after preincubating at 37°C for 1 min. The kinetic constants for glucuronidation of 1′-hydroxyestragole were determined at substrate concentrations that ranged from 50 to 2000μM 1′-hydroxyestragole. The reactions were terminated after 360 min by addition of 50 μl cold acetonitrile. Under these conditions glucuronidation of 1′-hydroxyestragole was linear with time and microsomal protein concentration. All samples were centrifuged for 5 min at 16,000 × g and 50 μl of the supernatant of each sample was analyzed by HPLC as described previously (Punt *et al.*, 2008). Formation of 1′-hydroxyestragole glucuronide in these incubations was verified by treatment of samples with β-glucuronidase and analysis of samples by liquid chromatography mass spectrometry (LC-MS) as described previously (Punt *et al.*, 2008). No synthetic standard of 1′-hydroxyestragole glucuronide was available for quantification of this conjugate. Because 1′-hydroxyestragole glucuronide has the same UV spectrum as 1′-hydroxyestragole (data not shown) it was assumed that it has the same molar extinction coefficient as 1′-hydroxyestragole, allowing quantification of this metabolite by comparison of the peak area of 1′-hydroxyestragole glucuronide in the chromatograms obtained at a wavelength of 225 nm to the calibration curve of 1′-hydroxyestragole. This calibration curve was prepared with the synthesized 1′-hydroxyestragole, which was analyzed by HPLC on an Alltima C18 5-μm

column, 150 mm × 4.6 mm (Alltech, Breda, The Netherlands) coupled to a Waters 2695 alliance HPLC system (Waters, Etten-Leur, the Netherlands). An isocratic mobile phase gradient was applied consisting of 25% acetonitrile and 75% ultrapure water containing 0.1% (vol/vol) acetic acid.

Oxidation of 1′-hydroxyestragole. Formation of 1′-oxoestragole was analyzed in incubations with both human and male rat liver microsomes, using NAD^{+} as cofactor and GSH to trap the transient 1′-oxoestragole. The kinetic constants for formation of the 1′-oxoestragole adduct with glutathione, reflecting the formation of 1′-oxoestragole were determined with human but also with male rat liver microsomes at substrate concentrations that ranged from 10 to 1000μM 1′-hydroxyestragole. These incubation mixtures had a final volume of 100 μl, containing (final concentrations) 3mM NAD^{+}, 2mM GSH, and 1 mg/ml microsomal protein in 0.2M Tris-HCl (pH 7.4). The reactions were terminated after 10 min by addition of 25 μl cold acetonitrile. Under these conditions the formation of the glutathione adduct, 3′-(glutathion-S-yl)-1′-oxo-2′-3′-dihydroestragole (GS-1′-oxoestragole), was linear with time and microsomal protein concentration. The level of GSH in the incubations was optimized to obtain maximum scavenging of 1′-oxoestragole. To this end incubations were performed in the presence of increasing concentrations of GSH, ranging from 2 to 10mM. At a concentration of 2mM GSH maximum formation of GS-1′-oxoestragole was reached in the incubations, pointing at maximum scavenging of 1′-oxoestragole at this concentration.

Due to the presence of microsomal protein in the incubations the maximum formation of GS-1′-oxoestragole could be affected by providing an alternative reaction possibility for the reactive 1′-oxoestragole. Experiments, in which the protein content was increased by addition of BSA revealed, however, no decrease in formation of GS-1′-oxoestragole, indicating that at a level of 1 mg/ml microsomal protein the protein content does not significantly decrease GS-1′-oxoestragole formation (data not shown).

For HPLC analysis the samples were centrifuged for 5 min at 16,000 × g and 50 μl of the supernatant of each sample was analyzed on an Alltima C18 5-μm column, 150 mm x 4.6 mm (Alltech) coupled to a Waters 2695 alliance HPLC system (Waters). The gradient was made with acetonitrile and ultrapure water containing 0.1% (vol/vol) acetic acid. The flow rate was 1 ml/min and a gradient was applied from 0 to 25% acetonitrile over 5 min, after which the percentage of acetonitrile was kept at 25% for 5 min and then increased to 100% over 2 min. Detection was performed at 280 nm using a Waters 2996 photodiode array detector (Waters).

Formation of GS-1′-oxoestragole in the incubations was verified by LC-MS, which was performed on a Finnigan Surveyor HPLC system coupled to an LXQ mass spectrometer (Thermo Finnigan, San Jose, CA). Aliquots of 20 μl (injected volume) were separated on an Alltima C18 5-μm column, 150 x 2.1 mm (Alltech). The gradient was made with acetonitrile and ultra pure water containing 0.1% (vol/vol) acetic acid and the flow rate was set to 0.1 ml/min. A linear gradient was applied from 0 to 25% acetonitrile over 5 min and was kept at 25% for 5 min, after which the percentage of acetonitrile was increased to 100% over 2 min. Mass spectrometric analysis was performed in positive electrospray mode using a spray voltage of 5 kV, a capillary temperature of 275°C, and nitrogen as sheath gas (60 arbitrary units). Full scan data (*m/z* 125–500) were obtained to identify the main protonated molecular ion (MH[+]) present in the sample.

Quantification of GS-1′-oxoestragole was performed by means of a calibration curve. To this end GS-1′-oxoestragole was synthesized as a reference compound from 1′-oxoestragole and GSH based on the protocol of Phillips *et al.* (1981). 1′-Oxoestragole was synthesized from 1′-hydroxyestragole as described for 1′-oxosafrole by Fennell *et al.* (1984). A calibration curve of GS-1′-oxoestragole was prepared by incubating 40μM 1′-oxoestragole with different concentrations of GSH, ranging from 2 to 20μM in 0.2M Tris-HCl (pH 7.4). The reactions were incubated for 4 h at 37°C resulting in maximum formation of GS-1′-oxoestragole. The peak area of GS-1′-oxoestragole in the chromatograms of these reactions were related to the quantity of GSH used in the reactions. This could be done because, according to both LC-MS analysis as well as HPLC analysis of the reaction mixture of GSH with 1′-oxoestragole, only one product is formed and there is no residual GSH (determined using

a GSH assay kit), indicating that all GSH has reacted and that, thus, the concentration of the adduct formed equals the original GSH concentration.

Kinetic analysis. The estragole concentration dependent rate of formation of different phase I metabolites and the 1′-hydroxyestragole concentration dependent glucuronidation and formation of 1′-oxoestragole were fitted to the standard Michaelis-Menten equation:

$$v = V_{max}/(1 + (K_m/[S]))$$

with [S] being the substrate concentration. The apparent maximum velocity ($V_{max(app)}$), the apparent Michaelis-Menten constant ($K_{m(app)}$), and the catalytic efficiency $V_{max(app)}/K_{m(app)}$ were determined, using the Life Science Workbench data analysis toolbox (version 1.1.1, MDL Information Systems, Inc. (San Leandro, CA)).

PBBK model. A PBBK model for estragole in human was developed based on the *in vitro* metabolic data. The model structure is similar to the structure of the PBBK model previously developed for estragole in male rat (Punt *et al.*, 2008), and includes compartments for blood, liver, lung, kidney, fat, rapidly perfused tissue, and slowly perfused tissue. The lung and kidney compartment were added to obtain an equal structure of the model compared with the previously developed model for estragole in male rat (Punt *et al.*, 2008). However, no specific reactions for absorption, metabolism, or excretion were defined in these compartments because, in contrast to rat samples, human microsomal incubations revealed no significant phase I metabolism of estragole in these tissues. A schematic diagram of the human PBBK model is shown in Figure 2. The physiological parameters and partition coefficients used in the model are given in Table 1. The physiological parameters were obtained from Brown *et al.* (1997). The partition coefficients were estimated from the log K_{ow} based on a method of DeJongh *et al.* (1997). Log K_{ow} values were estimated with the software package ClogP version 4.0 (Biobyte, Claremont, CA), and amounted to 3.1 for estragole and 1.6 for 1′-hydroxyestragole.

Based on *in vitro* conversion data (see Results section), conversion of estragole to 4-allylphenol, 1′-hydroxyestragole, estragole-2′,3′-oxide, and 3′-hydroxyanethole was described in the liver compartment. The apparent *in vitro* V_{max} values for these reactions, expressed as nmol min^{−1} (mg microsomal protein)[−1], were scaled to the liver using a microsomal protein yield of 32 mg/g liver (Barter *et al.*, 2007). The apparent *in vitro* K_m values were assumed to correspond to the apparent *in vivo* K_m values. The uptake of estragole from the gastrointestinal tract was described by a first-order process, assuming direct entry from the intestine to the liver compartment. The absorption rate constant (k_a) was 1.0 /h. Mass balance equations for estragole in the liver were similar to those described previously in the PBBK model for estragole in male rat (Punt *et al.*, 2008).

In the case of 4-allylphenol, estragole-2′,3′-oxide, and 3′-hydroxanethole only formation of these metabolites are taken into account, and no further reactions with these metabolites were modeled. Formation of 1′-hydroxyestragole was followed by additional metabolic reactions. To this end a near quantitative intrahepatic conversion of 1′-hydroxyestragole was assumed. This assumption was based on the findings that the overall catalytic efficiency for the reactions converting 1′-hydroxyestragole was higher than the catalytic efficiency for the formation of 1′-hydroxyestragole. This simplification of the model reduced the number of parameters considerably. Confining 1'-hydroxyestragole to the liver did not affect the relative formation of different metabolites or the area under the concentration time-curve of 1'-hydroxyestragole in the liver. The kinetic constants for glucuronidation of 1′-hydroxyestragole and formation of 1′-oxoestragole were determined in the present study, whereas the kinetic constants for sulfonation of 1′-hydroxyestragole were obtained from Punt *et al.* (2007). The apparent *in vitro* V_{max} values for glucuronidation and formation of 1′-oxoestragole, expressed as nmol min^{−1} (mg microsomal protein)[−1], were scaled to the liver using a microsomal protein yield of 32 mg per g liver (Barter *et al.*, 2007). The apparent *in vitro* V_{max} value for sulfonation of 1′-hydroxyestragole, expressed as nmol min^{−1} (mg S9 protein)[−1], were scaled to the liver using an S9 protein yield of 143 mg/g liver (Medinsky *et al.*, 1994). Mass balance equations for 1′-hydroxyestragole in the liver were similar to those described previously in the PBBK model for estragole in male rat (Punt *et al.*,
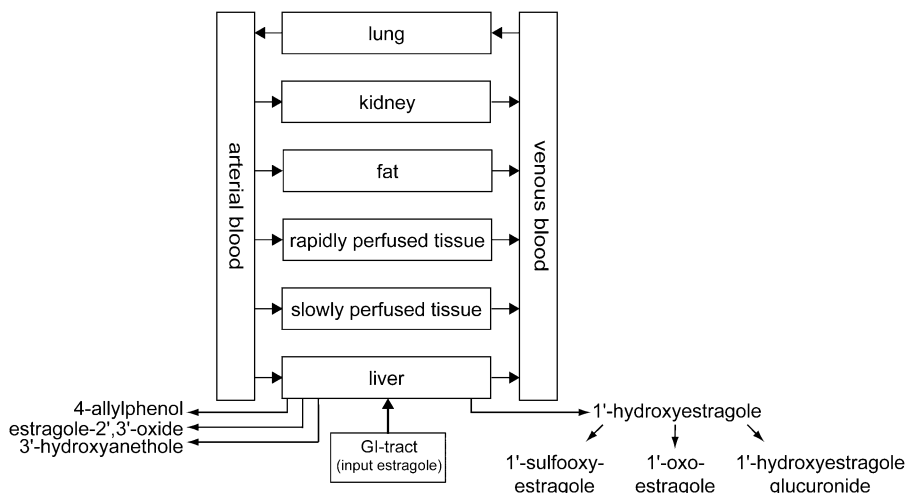
FIG. 2. Schematic diagram of the proposed PBBK model for estragole in human. The lung and kidney compartments were included in the model to obtain an equal structure of the model compared with the previously developed model for estragole in male rat (Punt *et al.*, 2008). However, no specific reactions for absorption, metabolism, or excretion of estragole were defined for these compartments.

2008), with the addition of oxidation of 1′-hydroxyestragole as additional metabolic route by adding the following term to the equation describing the rate of change in amount of 1′-hydroxyestragole in the liver compartment (dAL_{HE}/dt):

$$-V_{max, L\_OE} \times CL_{HE}/PL_{HE}/\left(K_{m, L\_OE} + CL_{HE}/PL_{HE}\right)$$

where AL_{HE} is the amount of 1′-hydroxyestragole in the liver (μmol), CL_{HE} is the 1′-hydroxyestragole concentration in the liver (μmol/l), PL_{HE} is the liver:blood partition coefficient of 1′-hydroxestragole, and V_{max,L_OE} and K_{m,L_OE} are the maximum rate of formation and the Michaelis-Menten constant for the formation 1′-oxoestragole in the liver.

Model equations were coded and numerically integrated in Berkeley Madonna 8.0.1 (Macey and Oster, UC Berkeley, CA), using the Rosenbrock′s algorithm for stiff systems. With the model obtained, predictions were made on the time-dependent concentrations of estragole and 1′-hydroxyestragole in human liver. In addition, predictions were made on the formation of different metabolites of both estragole and 1′-hydroxyestragole after 24 h (expressed as nmol/kg bw or percentage of the dose) following oral exposure to 0.07 mg/kg bw estragole and in case of 1′-sulfooxyestragole also at different oral dose levels. Additional predictions were made on the systemic bioavailability of estragole as an indication of the systemic levels of estragole available for extrahepatic metabolic conversion. The systemic bioavailability (BIO) of estragole was defined using the following equation:

$$BIO(\%) = Dose\,(i.v.)/Dose\,(oral) \times AUC\,(oral)/AUC\,(i.v.) \times 100$$

where AUC_{0-24} (oral dose) is the area under the concentration-time curve of the venous blood compartment after an oral dose of 0.07 mg/kg bw and AUC_{0-24} (i.v. dose) is the area under the concentration-time curve of the venous blood compartment after an intravenous dose of 0.07 mg/kg bw. The intravenous dose was applied in the venous blood compartment over a time period of 0.01 h.

Sensitivity analysis. A sensitivity analysis was performed to evaluate the relative effect of model parameters on the model output. Normalized sensitivity coefficients (SCs) were determined for the model parameters according to the following equation:

$$SC = (C' - C)/(P' - P) \times (P/C)$$

where C is the initial value of the model output, C' is the modified value of the model output resulting from an increase in parameter value, P is the initial parameter value, and P' is the modified parameter value (Evans and Andersen, 2000). Based on the literature (Evans and Andersen, 2000) a 5% increase in

parameter value was chosen to analyze the effect of a change in parameter value on the amount of 1′-hydroxyestagole and 1′-sulfooxyestragole (expressed as nmol/kg bw) formed over 24 h. Each parameter was analyzed individually, keeping the other parameters to their initial values. SCs were calculated for all physiological parameters (bw, tissue volumes, and blood flow rates), partition coefficients, and biochemical parameters (K_m and V_{max} values for the different metabolic reactions and k_a).

Results

Conversion of Estragole: Phase I Metabolism

HPLC analysis of incubations with human liver, lung, kidney, and small intestine microsomes in the presence of estragole as substrate and NADPH as cofactor reveals that conversion of estragole to phase I metabolites only occurs in incubations with human liver microsomes (Fig. 3A). No conversion of estragole is observed in incubations with microsomes from the other organs (data not shown). In the chromatograms of the incubations with human liver microsomes the peaks at 18.9, 20.6, and 39.6 min were identified as 1′-hydroxyestragole, 3′-hydroxyanethole, and 4-allylphenol on the basis of comparison of the retention times and UV spectra to the chemically synthesized reference compounds. The peak at 9.1 min was previously identified as estragole-2′,3′-diol (Punt *et al.*, 2008), which is formed upon hydrolysis of estragole-2′,3′-oxide due to the presence of epoxide hydrolases in human liver microsomes (Guenthner and Luo, 2001; Luo *et al.*, 1992).

Figure 3B shows the rate of formation of 1′-hydroxyestragole, estragole-2′,3′-oxide, 3′-hydroxyanethole, and 4-allylphenol in incubations with human liver microsomes with increasing estragole concentrations. Table 2 summarizes the apparent K_m and V_{max} values obtained from these plots as well as the catalytic efficiencies, calculated as V_{max}/K_m. In the

TABLE 1
Physiological Parameters and Partition Coefficients Used in the PBBK Model for Estragole in Human

Parameter	Value
Body weight (kg)[a]	60
Tissue volumes (% body weight)[a,b]	
Liver	2.6
Lungs	0.8
Kidneys	0.4
Fat	21.4
Rapidly perfused	4.2
Slowly perfused	54.3
Venous blood	5.92
Arterial blood	1.98
Cardiac output (l/h/kg bw$^{0.74}$)[a]	15
Blood flow to tissue (% cardiac output)[a]	
Liver	22.7
Kidneys	17.5
Fat	5.2
Rapidly perfused	29.8
Slowly perfused	24.8
Partition coefficients of estragole[c]	
Liver:blood	6.5
Lung:blood	6.5
Kidey:blood	6.5
Fat:blood	105
Rapidly perfused:blood	6.5
Slowly perfused:blood	4.1
Partition coefficient of 1′-hydroxyestragole[d]	
Liver:blood	1.6

[a]Brown *et al.* (1997).

[b]Does not account for hair, nails, and gut and bladder content.

[c]DeJongh *et al.* (1997).

[d]Used to determine the free concentration of 1′-hydroxyestragole in the liver available for metabolism.

FIG. 3. (A) Chromatographic profile of an incubation with human liver microsomes at a substrate concentration of 400 μM estragole, NADPH as cofactor and an incubation time of 10 min. Peaks marked with an asterisk were also present in the blank incubations performed without cofactor NADPH, in which they had the same area under the curve as in this incubation. (B) Estragole concentration dependent rate of formation of phase I metabolites by human liver microsomes. In the plots each point represents the mean (± SD) of three replicates corresponding to the formation of respectively 1′-hydroxyestragole (filled triangle), estragole-2′,3′-oxide (x), 3′-hydroxyanethole (filled square), and 4-allylphenol (filled circle).

incubations with human liver microsomes, the catalytic efficiency for formation of 1′-hydroxyestragole was the highest, followed by that for formation of estragole-2′,3′-oxide and 3′-hydroxyanethole. Formation of 4-allylphenol was the least efficient catalytic phase I conversion in these incubations. The high catalytic efficiency for 1′-hydroxylation of estragole is mainly due to a relatively low K_m for this reaction, which was respectively 4-, 14-, and 17-fold lower than the K_m for epoxidation, *O*-demethylation and 3′-hydroxylation.

Conversion of 1′-hydroxyestragole: Formation of 1′-hydroxyestragole Glucuronide

Formation of the glucuronosyl conjugate of 1′-hydroxyestragole was analyzed in incubations with pooled human liver microsomes. Figure 4A shows an HPLC-chromatogram of such an incubation in the presence of 1′-hydroxyestragole as substrate and UDPGA as cofactor and reveals the formation of a metabolite of 1′-hydroxyestragole with a retention time of 18.9 min. Treatment of the sample with β-glucuronidase resulted in complete elimination of this metabolite and
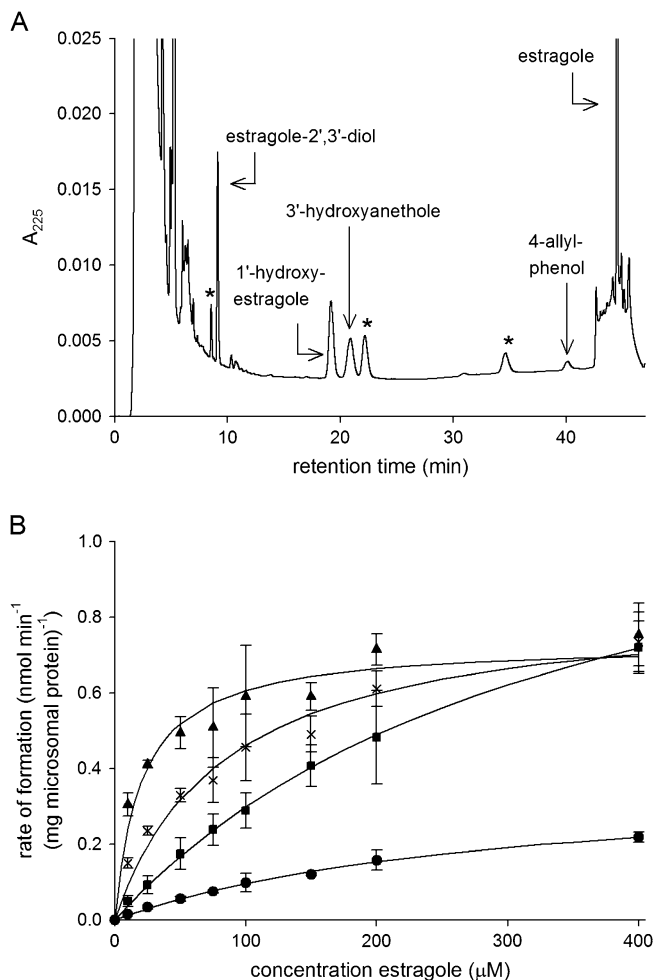
formation of a corresponding amount of 1′-hydroxyestragole (data not shown). This enzymatic deconjugation with β-glucuronidase together with LC-MS analysis of the metabolite, revealing a deprotonated molecule at *m/z* 339, which corresponds to the theoretically expected mass of 1′-hydroxyestragole glucuronide, confirms the formation of 1′-hydroxyestragole glucuronide. The 1′-hydroxyestragole concentration dependent rate of formation of 1′-hydroxyestragole glucuronide by human liver microsomes is displayed in Figure 4B. The kinetic constants were obtained from the graph by fitting the data to the standard Michaelis-Menten equation, resulting in an apparent K_m of 708μM and an apparent V_{max} of 0.3 nmol min^{-1} (mg microsomal protein)$^{-1}$.

TABLE 2
Kinetic Parameters for Phase I Metabolism of Estragole by
Human Liver Microsomes

Metabolite	$K_{m(app)}$[a,b]	$V_{max\ (app)}$[a,c]	*In vitro* catalytic efficiency[d]
4-Allylphenol	290 ± 28	0.38 ± 0.02	1.3
1′-Hydroxyestragole	21 ± 6	0.73 ± 0.04	34.8
3′-Hydroxyanethole	350 ± 20	1.35 ± 0.05	3.9
Estragole-2′,3′-oxide	83 ± 17	0.85 ± 0.07	10.2

[a]Mean ± SE.
[b]μM.
[c]nmol min^{-1} (mg microsomal protein)$^{-1}$.
[d]μl min^{-1} (mg microsomal protein)$^{-1}$ ($V_{max\ (app)}/K_{m(app)} \times 1000\ \mu$l/ml).

Conversion of 1′-hydroxyestragole: Formation of 1′-oxoestragole

In addition to conjugation reactions of 1′-hydroxyestragole the occurrence of oxidation of 1′-hydroxyestragole to 1′-oxoestragole was examined. Formation of this metabolite was observed in incubations with human liver microsomes using NAD$^+$ as cofactor and GSH to trap the transient 1′-oxoestragole. Figure 5A shows a HLC-chromatogram of such an incubation. The peak at 7.9 min was identified as GS-1′-oxoestragole on the basis of comparison of the retention time and UV spectrum to the chemically synthesized GS-1′-oxoestragole. Furthermore the mass spectrum of the metabolite, obtained by LC-MS, reveals a protonated molecule at m/z 470, which corresponds to the theoretically expected mass and this confirms formation of GS-1′-oxoestragole in the incubation. The peak was not present in the incubations without GSH or blank incubations without microsomes or cofactor (data not shown). Because the occurrence of this reaction was previously not analyzed for male rat (Punt *et al.*, 2008), additional incubations were performed to determine formation of 1′-oxoestragole by male rat liver microsomes as well. Figure 5B reveals the 1′-hydroxyestragole concentration dependent formation of 1′-oxoestragole by human and male rat liver microsomes as determined by quantification of the GS-1′-oxoestragole, which is assumed to represent the formation of 1′-oxoestragole. The K_m for formation of 1′-oxoestragole by human liver microsomes was determined to be 354μM and the V_{max} 4.9 nmol min^{-1} (mg microsomal protein)$^{-1}$. For formation of 1′-oxoestragole by rat liver microsomes the K_m was determined to be 1609 μM and the V_{max} 2.9 nmol min^{-1} (mg microsomal protein)$^{-1}$.

Comparison of the Kinetic Data for Estragole Bioactivation and Detoxification by Human and Male Rat Tissue Fractions

Table 3 presents a summary of the kinetic parameters for estragole bioactivation and detoxification by human tissue fractions combined with the kinetic parameters previously
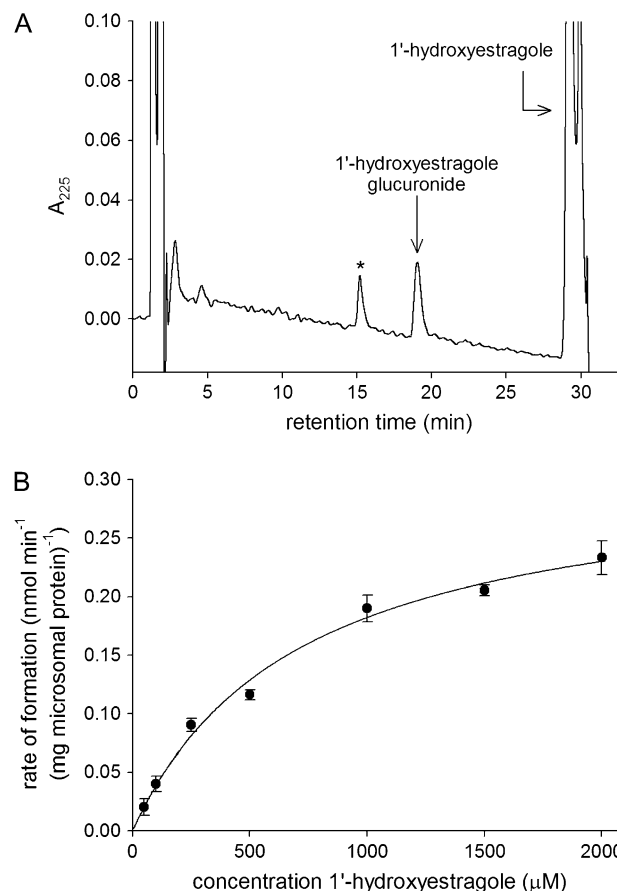

FIG. 4. (A) Chromatographic profile of an incubation with human liver microsomes at a substrate concentration of 500μM 1′-hydroxyestragole, UDPGA as cofactor and an incubation time of 360 min. The peak marked with an asterisk was also present in the blank incubation performed without cofactor. (B) 1′-Hydroxyestragole concentration dependent rate of formation of 1′-hydroxyestragole glucuronide by human liver microsomes. In the plot, each point represents the mean (± SD) of three replicates.

reported for male rat tissue fractions (Punt *et al.*, 2007, 2008). Available literature data on the kinetics for glucuronidation of 1′-hydroxyestragole by Iyer *et al.* (2003) were not included in this comparison, because we have previously observed that these data reflect kinetic constants for glucuronidation of 3′-hydroxyanethole rather than glucuronidation of 1′-hydroxyestragole (Punt *et al.*, 2008).

In Table 3, the V_{max} values expressed as μmol h^{-1} (g liver)$^{-1}$ were obtained by scaling of the *in vitro* V_{max} values to V_{max} values expressed per g liver using microsomal and S9 protein yields from the different organs that were obtained from the literature (Barter *et al.*, 2007; Medinsky *et al.*, 1994). This conversion allowed comparison of the kinetic constants obtained with different tissue fractions. In the case of phase I metabolism of estragole, comparison of the kinetic constants between humans and male rats reveals that the catalytic efficiency (scaled V_{max}/K_m) for formation of the proximate carcinogenic metabolite 1′-hydroxyestragole is 2.7-fold higher in human liver. Although
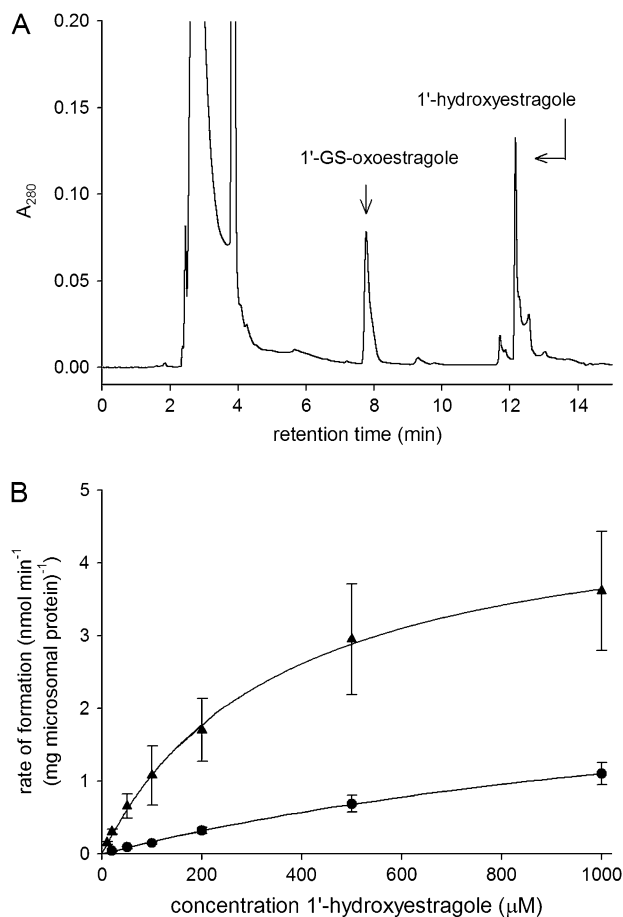
FIG. 5. (A) Chromatographic profile of an incubation with human liver microsomes at a substrate concentration of 500μM 1′-hydroxyestragole, NAD$^+$ as cofactor and GSH to trap the transient 1′-oxoestragole at an incubation time of 10 min. (B) 1′-Hydroxyestragole concentration dependent rate of formation of 1′-oxoestragole by human (filled triangle) and male rat (filled circle) liver microsomes as determined by quantification of the GS-1′-oxoestragole, which is assumed to represent the formation of 1′-oxoestragole. In the plots each point represents the mean (± SD) of three replicates.

the V_{max} for 1′-hydroxylation is twofold lower in human liver, the K_m is 5.5-fold lower resulting in a higher overall catalytic efficiency. The catalytic efficiencies for O-demethylation and epoxidation of estragole are similar for human and male rat liver, but the catalytic efficiency for 3′-hydroxylation of estragole is threefold lower in human liver. This lower observed catalytic efficiency is mainly due to a 3.8-fold higher K_m for 3′-hydroxylation in human liver. Another important difference between human and male rat is that no detoxifying O-demethylation occurs in human lung and kidney, whereas this metabolic route occurs with high affinity in male rat lung and kidney.

With respect to the metabolic reactions with 1′-hydroxyestragole, the catalytic efficiency for formation of the ultimate carcinogenic metabolite, 1′-sulfooxyestragole was previously found to be 30-fold lower in human liver compared with male rat liver (Table 3) (Punt *et al.*, 2007). Comparison of the

catalytic efficiency for glucuronidation of 1′-hydroxyestragole by human and male rat liver samples reveals that this metabolic route is more than 438 times less efficient in the human liver, which is mainly due to an 100-fold lower V_{max} for glucuronidation in human liver. Oxidation of 1′-hydroxyestragole is found to be a major metabolic route in human liver. Comparison of the catalytic efficiency for formation of 1′-oxoestragole by human and male rat liver samples reveals that this metabolic route is 9-fold more efficient in the human liver, which can be explained by both a 1.7-fold higher V_{max} value and a 4.5-fold lower K_m value for 1′-hydroxyestragole oxidation in human liver.

Human PBBK Model

Based on the *in vitro* kinetic data for bioactivation and detoxification of estragole by human tissue fractions a PBBK model for estragole in human was developed. Figure 6 displays the time-dependent predicted concentrations of estragole in plasma and liver and the time-dependent predicted concentrations of 1′-hydroxyestragole in the liver following oral exposure to 0.07 mg/kg bw estragole, which corresponds to the average dietary human intake as estimated by the SCF (2001). The PBBK model predicts that both estragole and 1′-hydroxyestragole are metabolized within the 24-h timeframe. Accumulation of estragole or its reactive metabolites is therefore not expected to occur when a repeated dosing would be applied after 24 h. With the model obtained, estimations were made on the formation of different metabolites (Table 4). The major part of estragole is converted to 1′-hydroxyestragole (304 nmol/kg bw, corresponding to 64.4% of the dose). This metabolite is in turn predominantly converted to 1′-oxoestragole (294 nmol/g liver, corresponding to 62.3% of the dose). Due to this high level of formation of 1′-oxoestragole, formation of the ultimate carcinogenic metabolite, 1′-sulfooxyestragole is relatively low, with only 0.19% of the dose being converted to this metabolite.

Estimation of the formation of the proximate carcinogenic metabolite 1′-hydroxyestragole at different oral doses revealed that the relative formation of this metabolite decreases with increasing dose due to saturation of this metabolic route. However, the observed relative decrease in formation of 1′-hydroxyestragole was not substantial at doses relevant for dietary human intake, given that at a dose of 0.7 mg/kg bw (i.e., 10-fold higher than the estimated average dietary human intake), the percentage of the dose that is ultimately converted to 1′-hydroxyestragole is similar (63.9%) to the one at a dose of 0.07 mg/kg bw (64.4%). Only when a dose of 10 mg/kg bw is applied (i.e., 150-fold higher than the average dietary human intake) a decrease of approximately 10% of the percentage of the dose converted to 1′-hydroxyestragole was observed leading to a value of 56.9%. The relative decrease in formation of 1′-hydroxyestagole with increasing doses resulted in a concomitant decrease in formation of 1′-sulfooxyestragole,

TABLE 3
Kinetic Constants for Estragole Metabolism by Human and Male Rat Tissue Fractions

Metabolite	Organ	Human[a]			Male rat[b]		
		Scaled $V_{\mathrm{max\ (app)}}$[c]	$K_{\mathrm{m\ (app)}}$[d]	Catalytic efficiency[e]	Scaled $V_{\mathrm{max\ (app)}}$[c]	$K_{\mathrm{m\ (app)}}$[d]	Catalytic efficiency[e]
estragole metabolites							
4-allylphenol	Liver	0.7	290	2	1.6	458	3
	Lung	n.d.[f]	n.d.	–	0.8	0.5	1600
	Kidney	n.d.	n.d.	–	0.2	0.5	400
1′-hydroxyestragole	Liver	1.4	21	67	2.8	116	24
	Lung	n.d.	n.d.	–	0.5	26	18
	Kidney	n.d.	n.d.	–	0.1	22	4
3′-hydroxyanethole	Liver	2.6	350	7	2.0	93	22
estragole-2′,3′-oxide	Liver	1.6	83	19	4.1	154	27
1′-hydroxyestragole metabolites							
1′-sulfooxyestragole	Liver	0.06	727	0.1	0.2	63	3
1′-hydroxyestragole glucuronide	Liver	0.6	708	1	60	137	438
1′-oxoestragole	Liver	9.4	354	27	5.6	1609	3

[a]Data obtained from present study and Punt *et al.* (2007).
[b]Data obtained from Punt *et al.* (2007), Punt *et al.* (2008) and in the case of 1′-oxoestragole from the present study.
[c]Scaled $V_{\mathrm{max\ (app)}}$ expressed as μmol h^{-1} (g tissue)$^{-1}$, calculated from the *in vitro* $V_{\mathrm{max\ (app)}}$ based on a microsomal protein yield of 32, 20, and 7 mg/g tissue for liver, lung, and kidney respectively, and an S9 protein yield of 143 mg/g liver.
[d]$K_{\mathrm{m(app)}}$ expressed as μM.
[e]Catalytic efficiency (scaled $V_{\mathrm{max\ (app)}}/K_{\mathrm{m(app)}}$) expressed as ml h^{-1} (g liver)$^{-1}$.
[f]n.d. = not detectable.

1′-hydroxyestragole glucuronide, and 1′-oxoestragole amounting to respectively 0.19, 1.9, and 61.8% of the dose at 0.7 mg/kg bw and to 0.17, 1.7, and 55.0% of the dose at 10 mg/kg bw.

The performance of the PBBK model defined for estragole in human could, to some extent, be evaluated against available *in vivo* data on the disposition of 0.001 mg/kg bw

FIG. 6. PBBK-model predicted time dependent concentrations of estragole in plasma and liver and the time-dependent predicted concentrations of 1′-hydroxyestragole in the liver following exposure to 0.07 mg/kg bw estragole.

[methoxy-^{14}C]-labeled estragole in two human volunteers obtained from Sangster *et al.* (1987). In this disposition study of estragole in humans, ~10% of the dose was excreted as ^{14}CO$_2$ after 8 h, corresponding to the level of *O*-demethylation of estragole. The major part of the radioactivity (31–37% of the dose after 8 h, 47–53% after 24 h, and 54–62% after 48 h) was excreted in the urine, corresponding to metabolites arising from various oxidations of the side chain (Sangster *et al.*, 1987). Structural analysis of the urinary metabolites revealed ~0.4% of the dose being excreted as 1′-hydroxyestragole glucuronide. For evaluation of the model performance, the PBBK-model predicted formation of 1′-hydroxyestragole glucuronide and 4-allylphenol, at an oral
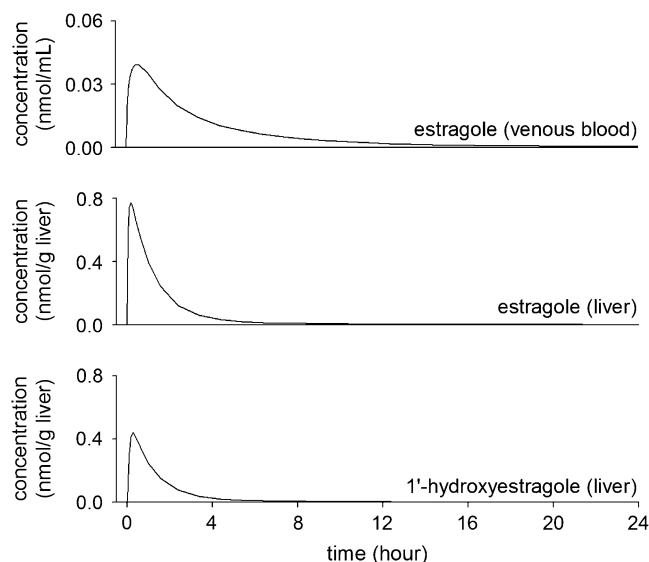
TABLE 4
PBBK-model Predicted Quantities of Metabolites Formed During 24 h After an Oral Dose of 0.07 mg/kg bw (472 nmol/kg bw)

Metabolite	Amount formed (nmol/kg bw)
Estragole metabolites	
4-Allylphenol	12
1′-Hydroxyestragole	304
3′-Hydroxyanethole	34
Estragole-2′,3′-oxide	90
1′-Hydroxyestragole metabolites	
1′-Hydroxyestragole glucuronide	9
1′-Oxoestragole	294
1′-Sulfooxyestragole	0.9

dose of 0.001 mg/kg bw, were compared with the reported levels of these metabolites. To this end it was assumed that formation of 1′-hydroxyestragole glucuronide equals excretion of this metabolite in the urine, whereas formation of 4-allylphenol is assumed to correspond to the reported level of exhalation of $^{14}CO_2$. The PBBK-model predicted formation of 1′-hydroxyestragole glucuronide, corresponding to 1.9% of the dose after 24 h, is 5-fold higher than the reported *in vivo* level of this metabolite of ~0.4%. The predicted formation of 4-allylphenol, corresponding to 2.4% of the dose after 8 h, is fourfold lower than the reported *in vivo* level of ~10% of the dose after 8 h (Sangster *et al.*, 1987). These results indicate that the PBBK model predicts the formation of these metabolites within the same order of magnitude as the reported levels. Formation of the major metabolite, 1′-oxoestragole, could not be evaluated against human *in vivo* data, since excretion of 1′-oxoestragole as GSH or protein adducts was not analyzed in humans exposed to estragole (Sangster *et al.*, 1987).

Sensitivity Analysis

The sensitivity of the predicted formation of 1′-hydroxyestragole and 1′-sulfooxyestragole to changes in all model parameters was analyzed to identify the key parameters in the human model that influence bioactivation of estragole. Normalized SCs were calculated at a dose of 0.07 mg/kg bw estragole, but only parameters that had a normalized SC higher than 0.1 (in absolute value) are displayed in Figure 7. Formation of 1′-hydroxyestragole is influenced by the kinetic constants for 1′-hydroxylation of estragole in the liver and to a minor extent also by the kinetic constants for epoxidation, which is the most important competing metabolic pathway to 1′-hydroxylation in the liver. In the case of 1′-sulfooxyestragole, the predicted formation of this metabolite depends on the parameters that determine the formation of 1′-hydroxyestragole, but formation of this metabolite is predominantly influenced by the kinetic constants for the formation of 1′-oxoestragole and the kinetic constants for formation of 1′-sulfooxyestragole itself. This indicates that oxidation of 1′-hydroxyestragole is an important competing metabolic pathway to sulfonation due to its higher catalytic efficiency. Physiological parameters (bw, tissue volumes, and blood flow rates) and partition coefficients do not significantly affect the relative extent of formation of 1′-hydroxyestragole and 1′-sulfooxyestragole in human liver. Differences in, for instance, estimated tissue:blood partition coefficients between human and rat will therefore not affect the comparison between these species in formation of 1′-hydroxyestragole and 1′-sulfooxyestragole.

Comparison of the PBBK-Model Predicted Plasma and Tissue Levels of Estragole and 1′-hydroxyestragole between Human and Male Rat

To obtain insight in possible species differences in metabolic activation and detoxification of estragole between human and
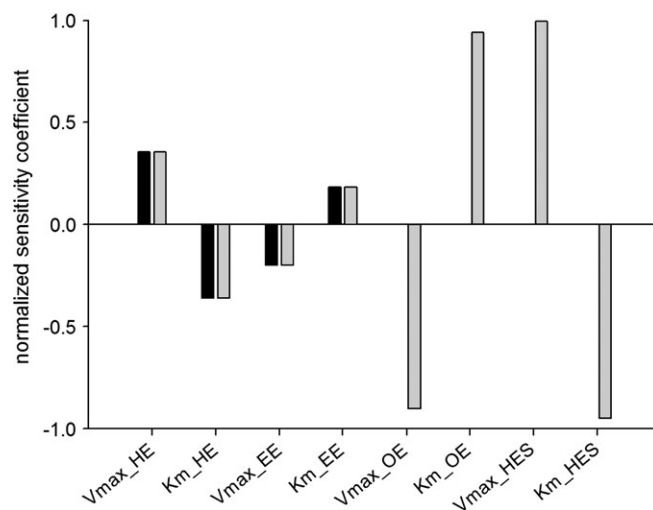

FIG. 7. Sensitivity of the predicted formation of 1′-hydroxyestragole (black bars) and 1′-sulfooxyestragole (gray bars) to different model parameters. The V_{max} and K_m correspond to the maximum rate of formation and the Michaelis-Menten constant for the formation of the different metabolites in the liver: 1′-hydroxyestragole (HE), estragole-2′,3′-oxide (EE), 1′-oxoestragole (OE) and 1′-sulfooxyestragole (HES).

male rat, the results obtained with the PBBK model for estragole in human were compared with those of the previously defined PBBK model for estragole in male rat (Punt *et al.*, 2008). Because the formation of 1′-oxoestragole from 1′-hydroxyestragole was previously not described in the PBBK model for male rat, the rat model was adjusted by the addition of this metabolic route using the kinetic data obtained in the present study to allow equal comparison between the rat and human model.

The predicted AUC_{0-24h} of estragole in plasma is predicted to be fourfold higher for human than for male rat (Fig. 8). This can be explained by the higher overall clearance of estragole in rat due to significant extrahepatic metabolism of estragole in male rat lung and kidney (Punt *et al.*, 2008), which does not occur in human lung and kidney. Comparison of the predicted AUC_{0-24h} of estragole in the liver between human and male rat reveals that the AUC_{0-24h} is sixfold higher in human. This is the result of a threefold higher value of the estimated partition coefficient of estragole in human liver. This phenomenon has previously been attributed to a higher solubility of lipophilic compounds in rat blood over human blood, which is assumed to be a result of species differences in the hemoglobin structure (Lam *et al.*, 1990; Wiester *et al.*, 2002). In case of 1′-hydroxyestragole, the AUC_{0-24h} of this metabolite in the liver is predicted to be 144-fold higher in human than in male rat, which can be explained by a higher level of formation of this metabolite as well as a lower metabolic clearance of this metabolite in human liver. Overall, the differences in plasma and liver levels of estragole and liver levels of 1′-hydroxyestragole indicate that the turnover of both estragole and 1′-hydroxyestragole is relatively lower in human compared with
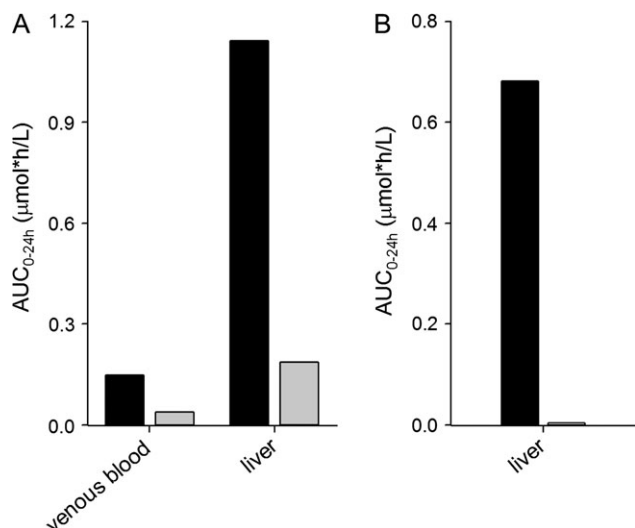
FIG. 8. PBBK-model predicted area under the concentration-time curve (AUC_{0-24h}) for estragole in plasma and liver (A) and 1′-hydroxyestragole (B) in human (black bars) and male rat (gray bars) in the liver following exposure to 0.07 mg/kg bw estragole.

male rat. These differences in turnover will affect the time-frame in which various metabolites are formed, but does not affect the relative levels, at which different metabolites are formed when metabolic conversion is completed.

Comparison of the PBBK-Model Predicted Formation of Metabolites between Human and Male Rat

Comparison of the PBBK-model predicted formation of different metabolites will provide an indication of the relative extent of bioactivation and detoxification of estragole. The evaluation of species differences in the formation of various metabolites, presented hereafter, is first focused on dose levels relevant for dietary human intake. In addition, a comparison is made between human and male rat in the predicted formation of 1′-sulfooxyestragole at different oral doses.

In Figure 9A the predicted formation of phase I metabolites (expressed as percentage of the dose) in human and male rat following an oral dose of 0.07 mg/kg bw estragole is displayed. A major difference between humans and male rats occurs in the formation of 4-allylphenol, which is predicted to be 24-fold lower in humans. This observed difference is due to the effect of extrahepatic metabolism on the formation of this metabolite, occurring in male rat (Punt *et al.*, 2008) but not in human. In male rat, first pass metabolism of estragole in the liver is relatively low, resulting in a relatively high systemic bio-availability of estragole, which is predicted to amount to 57% at a dose of 0.07 mg/kg bw. Extrahepatic conversion of estragole is therefore possible. Metabolism in the lung and kidney contribute significantly to the extent of O-demethyla-tion of estragole in male rat, since this reaction occurs in these organs with high affinity (Punt *et al.*, 2008). In humans, systemic availability of estragole is predicted to be 32% at

a dose of 0.07 mg/kg bw, which is lower than in male rat. But more importantly, no detoxifying O-demethylation, or other phase I metabolic reactions occur in human lung and kidney. Due to the lower extent of O-demethylation as well as a higher efficiency for 1′-hydroxylation in human, the formation of 1′-hydroxyestragole is observed to be fourfold higher in human compared with male rat. Formation of 3′-hydroxyanethole and estragole-2′,3′-oxide are similar in the two species.

Figure 9B displays the metabolites formed from 1′-hydroxyestragole in human and male rat. The greater part of the 1′-hydroxyestragole that is formed in human is oxidized to 1′-oxoestragole, which is due to the relative high efficiency for oxidation of 1′-hydroxyestragole in comparison to glucuroni-dation and sulfonation. When the oxidation of 1′-hydroxyes-tragole is added to the rat PBBK model, the model predicts low formation of this metabolite at a level corresponding to 0.1% of the dose. This is due to the fact that the catalytic efficiency for the formation of 1′-oxoestragole in male rat is much lower in comparison to glucuronidation of 1′-hydroxyestragole. In male rat 1′-hydroxyestragole is almost completely metabolized to 1′-hydroxyestragole glucuronide. Comparison of the predicted formation of the ultimate carcinogenic metabolite between human and male rat reveals that the predicted overall formation of 1′-sulfooxyestragole is approximately twofold higher in human liver at an oral dose of 0.07 mg/kg bw.

Because dose-dependent effects in bioactivation and de-toxification can affect the level of species differences at different oral doses, a comparison needs to be made on the predicted formation of 1′-sulfooxyestragole at different oral doses between human and male rat. The predicted formation of 1′-sulfooxyestragole, expressed as nmol/kg bw, within a dose range of 10^{-5} mg/kg bw and 10^{3} mg/kg bw is depicted in Figure 10. Both curves are observed to be quite linear up to doses as high as 100 mg/kg bw, when plotted on a log-log scale as done in Figure 9 as well as on a linear scale (not shown). In case of male rat, the previously predicted relative increase in formation of 1′-sulfooxyestragole with increasing doses (Punt *et al.*, 2008) is not significant enough to result in large species differences at higher dose levels. In case of human, saturation of the 1′-hydroxylation pathway at doses higher than 100 mg/kg bw results in a decrease in the relative formation of 1′-sulfooxyestragole with increasing doses. At these dose levels, formation of 1′-sulfooxyestragole becomes relatively lower in human compared with male rat.

Discussion

A PBBK model for estragole metabolism in human was defined based on *in vitro* kinetic data, providing possibilities to evaluate the relative extent of different metabolic routes at dose levels relevant for dietary human intake. With the model obtained, the occurrence of species differences in metabolic activation of estragole was evaluated by comparison of the

FIG. 10. PBBK model-predicted dose-dependent formation of 1′-sulfooxy-estragole in the liver of rat (—) and human (- -).
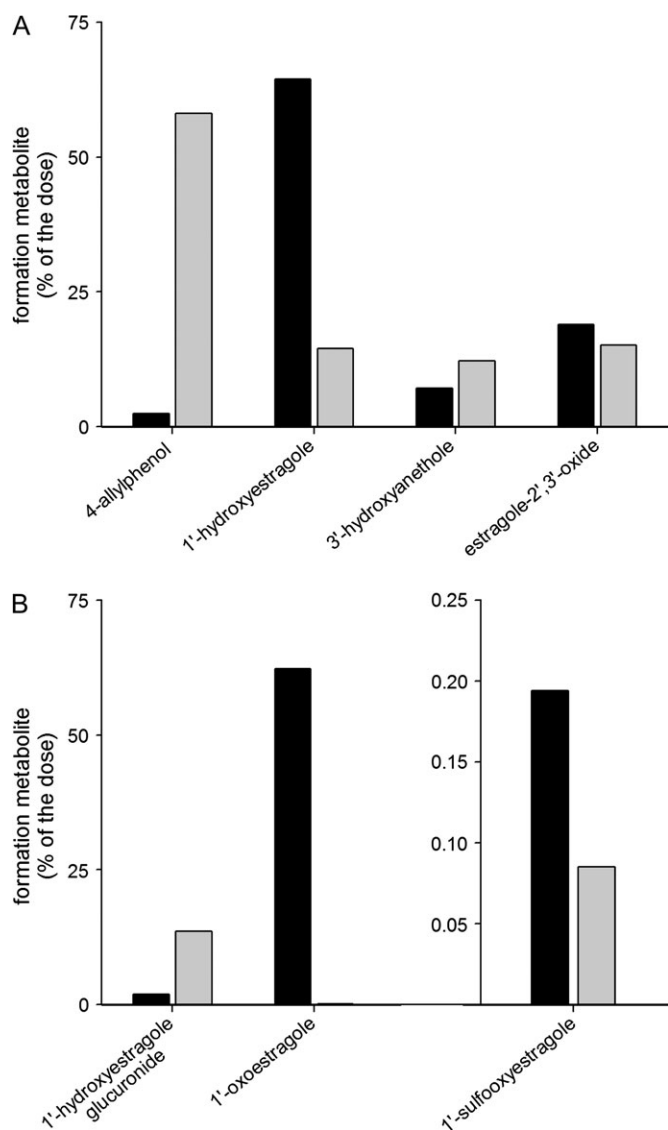

FIG. 9. PBBK-model predicted formation of phase I metabolites in human (black bar) and male rat (gray bar) following an oral dose of 0.07 mg/kg bw estragole (A) and the metabolites formed from 1′-hydroxyestragole in human and male rat at this oral dose (B).

modeling (Hissink *et al.*, 1997; Lupfert and Reichel, 2005; Quick and Shuler, 1999), and which might provide an indication that the critical metabolic pathways have been captured in the model. For a more complete evaluation of the performance of the model, however, additional *in vivo* data are needed, especially on the plasma levels of estragole and/or its metabolites. Overall, it should be stated that the present model derived from integrating *in vitro* metabolic data using PBBK modeling as a platform, does not allow conclusions based on absolute outcomes. However, the relative importance of different metabolic pathways in humans can be predicted and moreover a relative comparison of species differences in the extent of bioactivation and detoxification can be made, since the *in vitro* metabolic data for human and male rat are obtained with similar methods.

Based on the approach of identifying principal metabolic pathways of estragole in incubations with human tissue fractions, the present study revealed that oxidation of 1′-hydroxyestragole can be a main detoxification route of 1′-hydroxyestragole in humans. Formation of the major metabolite 1′-oxoestragole could, however, not be evaluated against human *in vivo* data, because excretion of this metabolite or its conjugates was not analyzed in humans exposed to estragole (Sangster *et al.*, 1987). In this study on humans exposed to estragole (Sangster *et al.*, 1987), the greater part of the urinary metabolites (36–44% of the oral dose) could not be identified due to insufficient knowledge of the nature of the excreted metabolites. In addition, a significant proportion of ~30% of the radioactivity was not recovered within 48 h (Sangster *et al.*, 1987). It was suggested by the authors that this incomplete recovery of radioactivity could be due to premature termination of the collection of exhaled $^{14}CO_2$ after 8 h, suggesting that metabolic conversion of estragole is not complete within this time-frame (Sangster *et al.*, 1987). The outcomes of the PBBK model of the present study indicate, however, that metabolic

outcomes of the defined model with those of the previously defined PBBK model for estragole in male rat (Punt *et al.*, 2008).

The performance of the human PBBK model was evaluated by comparing the predicted formation of 4-allylphenol and 1′-hydroxyestragole glucuronide to the reported levels of these metabolic routes in humans exposed to a single oral dose of estragole (Sangster *et al.*, 1987). The predicted formation of 4-allylphenol and 1′-hydroxyestragole glucuronide were in the same order of magnitude as the reported levels of these metabolic routes in humans exposed to estragole (Sangster *et al.*, 1987), which can be considered acceptable within the present state-of-the-art of integrating *in vitro* data and PBBK
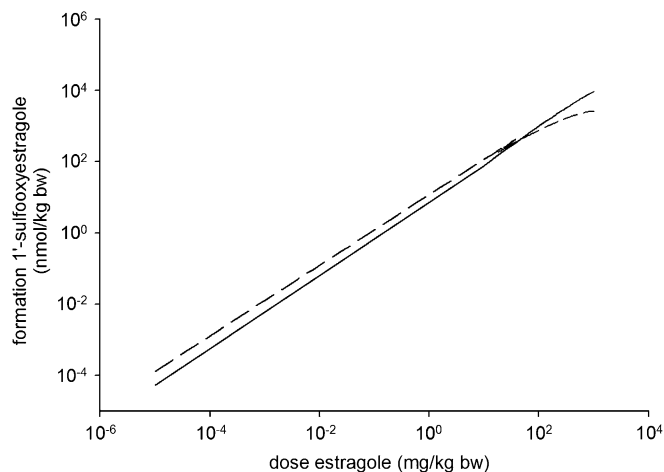
conversion of estragole is essentially complete within 8 h and might suggest another reason for incomplete recovery of radioactivity, which could, for instance, be due to enterohepatic circulation of metabolites. Overall, the large proportion of unidentified metabolites in humans might reflect the formation of 1′-oxoestragole, which was predicted to amount to 62.7% of the dose, based on the PBBK model for estragole in human developed in the present study. Obviously, the relevance of the oxidation pathway of 1′-hydroxyestragole in humans needs to be further confirmed *in vivo*.

Although the extent of oxidation of 1′-hydroxyestragole to 1′-oxoestragole could not be evaluated against human *in vivo* data, evidence for the presence *in vivo* of the oxidation route of 1′-hydroxyestragole can be found in experiments with rats exposed to estragole or other alkenylbenzenes. Solheim and Scheline (1973) described the excretion of small amounts of amino conjugates in rats exposed to estragole, which were assumed to originate from 1′-oxoestragole. In the case of the related alkenylbenzene safrole, Fennell *et al.* (1984) described the excretion of GS-1′-oxosafrole and N-acetylcystein-1′-oxosafrole in rats exposed to the 1′-hydroxy metabolite of this compound, indicating formation of 1′-oxo metabolites in these rats. The excretion of 1′-oxosafrole conjugates was however relatively low in comparison to the excretion of glucuronosyl conjugates of 1′-hydroxysafrole, which is in agreement with results of the present study revealing that the predicted formation of 1′-oxoestragole is relatively low and of minor importance in male rat in comparison to the predicted glucuronidation of 1′-hydroxyestragole. Although 1′-oxoestragole can potentially react with DNA (Phillips *et al.*, 1981), this metabolite, which is a soft acid, is not expected to contribute to the genotoxicity of estragole *in vivo*, since it can readily react with glutathione (soft base) rather than with DNA molecules (hard bases) (Fennell *et al.*, 1984). This is supported by literature data revealing that 1′-oxoestragole is not carcinogenic *in vivo* in mice (Wiseman *et al.*, 1987). For this reason formation of 1′-oxoestragole in human can be considered as the major detoxification pathway of 1′-hydroxyestragole.

Comparison of the predicted extent of bioactivation of estragole between humans and male rats at a dose of 0.07 mg/kg bw showed that the formation of the proximate carcinogenic metabolite 1′-hydroxyestragole is fourfold higher in human liver compared with male rat liver, which is mainly due to the relatively lower extent of detoxification of estragole through *O*-demethylation in human. This observation that *O*-demethylation of estragole is a less important metabolic route in humans than in rats is supported by *in vivo* data showing that only ~10% of the oral dose was excreted through this metabolic route in humans at a dose of 0.001 mg/kg bw (Sangster *et al.*, 1987), whereas in rats this metabolic route accounted for 53% of the oral dose at a comparable dose level of 0.05 mg/kg bw (Anthony *et al.*, 1987). The relatively high formation of the *O*-demethylated metabolite 4-allylphenol in

male rats at low dose levels has previously been demonstrated to be due to extrahepatic formation of 4-allylphenol in lung and kidney tissue of male rat at low oral doses of estragole (Punt *et al.*, 2008). Such a high level of extrahepatic metabolism of estragole in male rat is possible due to a relatively high systemic bioavailability of estragole and the capacity of the lung and kidney tissue to catalyze *O*-demethylation of estragole with a high affinity (Punt *et al.*, 2008).

No detoxifying *O*-demethylation or other phase I metabolic reactions were observed to occur in human lung and kidney tissue samples. The absence of phase I metabolism in human lung and kidney can be rationalized when the P450 enzymes involved are not expressed in these tissues. Jeurissen *et al.* (2007) recently identified that P450 1A2 and P450 2A6 play a pivotal role in estragole 1′-hydroxylation. These enzymes are absent or only poorly expressed in human lung and kidney (Pelkonen and Raunio, 1997; Shimada *et al.*, 1996), which is in line with the observation that no significant 1′-hydroxylation activity occurs in the corresponding tissue fractions. The P450 enzymes involved in *O*-demethylation have not been identified so far, but if it would be assumed that similar P450 enzymes as for 1′-hydroxylation are involved, this would explain that overall no phase I metabolism is detected in human lung and kidney tissue.

Mainly due to a lower level of *O*-demethylation of estragole in human compared with male rat, the predicted formation of 1′-hydroxyestragole (expressed as percentage of the dose) is fourfold higher in human. Even though formation of 1′-hydroxyestragole is fourfold higher, the formation of the ultimate carcinogenic metabolite, 1′-sulfooxyestragole is predicted to be only twofold higher in human. This can be explained by the fact that the major part of 1′-hydroxyestragole is oxidized to 1′-oxoestragole in human, due to a relative high catalytic efficiency for oxidation of 1′-hydroxyestragole. The twofold higher predicted formation of 1′-sulfooxyestragole in human as compared with rat liver was consistent over a dose-range from 10^{-5} to 10^{2} mg/kg bw. At higher doses the predicted formation of 1′-sulfooxyestragole can become 1.5 to 2-fold lower in human compared with male rat, mainly due to saturation of the 1′-hydroxylation pathway of estragole in humans, which results in a concomitant apparent saturation of the formation of 1′-sulfooxyestragole.

The observed species differences in bioactivation and detoxification of estragole, outlined above, reflect differences between male rat and an average human situation. Significant interindividual variation might, however, occur due to genotype- and lifestyle-based factors that influence the activity of enzymes for the key metabolic reactions involved in bioactivation and detoxification of estragole. Parameter sensitivity analysis of the predicted formation of 1′-sulfooxyestragole in humans revealed that formation of this metabolite mainly depends on the kinetics of formation of 1′-hydroxyestragole, subsequent oxidation of 1′-hydroxyestragole to 1′-oxoestragole, as well as the kinetics of the formation of 1′-sulfooxyestragole itself. Knowledge about

the enzymes involved in these reactions is essential to obtain insight in the consequences of possible interindividual variation in these enzymes. As indicated above, 1′-hydroxylation of estragole is mainly catalyzed by P450 1A2 and 2A6 (Jeurissen *et al*., 2007). The activities of these enzymes are known to be significantly affected by genotype- and lifestyle-based factors (Ingelman-Sundberg *et al*., 1999; Jiang *et al*., 2006). Additional studies are currently being performed to identify enzymes involved in other bioactivation and detoxification pathways of estragole and to determine the effect of interindividual variability in these metabolic reactions on the formation of the ultimate carcinogen, 1′-sulfooxyestragole. In the safety assessment of estragole these interindividual differences need to be taken into account.

When extrapolating cancer data from high dose animal experiments to the low dose human situation it is important to take species differences in metabolism and metabolic activation into account. Comparison of *in vitro* metabolic data for estragole bioactivation and detoxification between human and male rat, as done in the present study using PBBK modeling to integrate these metabolic data, provides an approach that allows to evaluate whether species differences in bioactivation are to be expected. Overall it is shown that, even though significant species differences in the relative extent of different metabolic pathways occur between human and male rat, these differences ultimately only result in a minor difference in the PBBK model based predicted formation of 1′-sulfooxyestragole at dose levels relevant for dietary human intake It is, therefore, concluded that in spite of significant differences in the catalytic efficiency of specific individual estragole bio-transformation reactions there is a minor influence of species differences between human and male rats on the ultimate overall bioactivation of estragole to its ultimate carcinogenic DNA reactive metabolite 1′-sulfooxyestragole.

FUNDING

REFERENCES

Anthony, A., Caldwell, J., Hutt, A. J., and Smith, R. L. (1987). Metabolism of estragole in rat and mouse and influence of dose size on excretion of the proximate carcinogen 1′-hydroxyestragole. *Food Chem. Toxicol.* **25**, 799–806.

Barter, Z. E., Bayliss, M. K., Beaune, P. H., Boobis, A. R., Carlile, D. J., Edwards, R. J., Houston, J. B., Lake, B. G., Lipscomb, J. C., Pelkonen, O. R., *et al*. (2007). Scaling factors for the extrapolation of in vivo metabolic drug clearance from in vitro data: Reaching a consensus on values of human microsomal protein and hepatocellularity per gram of liver. *Curr. Drug Metab.* **8**, 33–45.

Brown, R. P., Delp, M. D., Lindstedt, S. L., Rhomberg, L. R., and Beliles, R. P. (1997). Physiological parameter values for physiologically based pharma-cokinetic models. *Toxicol. Ind. Health* **13**, 407–484.

DeJongh, J., Verhaar, H. J. M., and Hermens, J. L. M. (1997). A quantitative property-property relationship (QPPR) approach to estimate *in vitro* tissue-blood partition coefficients of organic chemicals in rats and humans. *Arch. Toxicol.* **72**, 17–25.

Drinkwater, N. R., Miller, E. C., Miller, J. A., and Pitot, H. C. (1976). Hepatocarcinogenicity of estragole (1-allyl-4-methoxybenzene) and 1′-hydroxyestragole in the mouse and mutagenicity of 1′-acetoxyestragole in bacteria. *J. Natl. Cancer Inst.* **57**, 1323–1331.

Evans, M. V., and Andersen, M. E. (2000). Sensitivity analysis of a physiological model for 2,3,7,8-tetrachlorodibenzo-p-dioxin (TCDD): Assessing the impact of specific model parameters on sequestration in liver and fat in the rat. *Toxicol. Sci.* **54**, 71–80.

Fisher, M. B., Campanale, K., Ackermann, B. L., VandenBranden, M., and Wrighton, S. A. (2000). *In vitro* glucuronidation using human liver microsomes and the pore-forming peptide alamethicin. *Drug Metab. Dispos.* **28**, 560–566.

Guenthner, T. M., and Luo, G. (2001). Investigation of the role of the 2′,3′-epoxidation pathway in the bioactivation and genotoxicity of dietary allylbenzene analogs. *Toxicology* **160**, 47–58.

Hissink, A. M., Van Ommen, B., Kruse, J., and Van Bladeren, P. J. (1997). A physiologically based pharmacokinetic (PB-PK) model for 1,2-dichloroben-zene linked to two possible parameters of toxicity. *Toxicol. Appl. Pharmacol.* **145**, 301–310.

Ingelman-Sundberg, M., Oscarson, M., and McLellan, R. A. (1999). Polymorphic human cytochrome P450 enzymes: An opportunity for individualized drug treatment. *Trends Pharmacol. Sci.* **20**, 342–349.

Iyer, L. V., Ho, M. N., Shinn, W. M., Bradford, W. W., Tanga, M. J., Nath, S. S., and Green, C. E. (2003). Glucuronidation of 1′-hydroxyestragole (1′-HE) by human UDP-glucuronosyltransferases UGT2B7 and UGT1A9. *Toxicol. Sci.* **73**, 36–43.

Jeurissen, S. M., Punt, A., Boersma, M. G., Bogaards, J. J. P., Fiamegos, Y. C., Schilter, B., Van Bladeren, P. J., Cnubben, N. H. P., and Rietjens, I. M. C. M. (2007). Human cytochrome P450 enzyme specificity for the bioactivation of estragole and related alkenylbenzenes. *Chem. Res. Toxicol.* **20**, 798–806.

Jiang, Z., Dragin, N., Jorge-Nebert, L. F., Martin, M. V., Guengerich, F. P., Aklillu, E., Ingelman-Sundberg, M., Hammons, G. J., Lyn-Cook, B. D., Kadlubar, F. F., *et al*. (2006). Search for an association between the human CYP1A2 genotype and CYP1A2 metabolic phenotype. *Pharmacogenet. Genomics* **16**, 359–367.

Lam, C. W., Galen, T. J., Boyd, J. F., and Pierson, D. L. (1990). Mechanism of transport and distribution of organic solvents in blood. *Toxicol. Appl. Pharmacol.* **104**, 117–129.

Lin, J. H., and Wong, B. K. (2002). Complexities of glucuronidation affecting *in vitro in vivo* extrapolation. *Curr. Drug Metab.* **3**, 623–646.

Luo, G., Qato, M. K., and Guenthner, T. M. (1992). Hydrolysis of the 2′,3′-allylic epoxides of allylbenzene, estragole, eugenol, and safrole by both microsomal and cytosolic epoxide hydrolases. *Drug Metab. Dispos.* **20**, 440–445.

Lupfert, C., and Reichel, A. (2005). Development and application of physiologically based pharmacokinetic-modeling tools to support drug discovery. *Chem. Biodivers.* **2**, 1462–1486.

Medinsky, M. A., Leavens, T. L., Csanady, G. A., Gargas, M. L., and Bond, J. A. (1994). In vivo metabolism of butadiene by mice and rats: A comparison of physiological model predictions and experimental data. *Carcinogenesis* **15**, 1329–1340.

Miller, E. C., Swanson, A. B., Phillips, D. H., Fletcher, T. L., Liem, A., and Miller, J. A. (1983). Structure-activity studies of the carcinogenicities in the mouse and rat of some naturally occurring and synthetic alkenylben-zene derivatives related to safrole and estragole. *Cancer Res.* **43**, 1124–1134.

Pelkonen, O., and Raunio, H. (1997). Metabolic activation of toxins: tissue-specific expression and metabolism in target organs. *Environ. Health Perspect.* **105**(Suppl. 4), 767–774.

Phillips, D. H., Miller, J. A., Miller, E. C., and Adams, B. (1981). Structures of the DNA adducts formed in mouse liver after administration of the proximate hepatocarcinogen 1′-hydroxyestragole. *Cancer Res.* **41**, 176–186.

Phillips, D. H., Reddy, M. V., and Randerath, K. (1984). ^{32}P-post-labelling analysis of DNA adducts formed in the livers of animals treated with safrole, estragole and other naturally-occurring alkenylbenzenes. II. Newborn male B6C3F1 mice. *Carcinogenesis* **5**, 1623–1628.

Punt, A., Delatour, T., Scholz, G., Schilter, B., Van Bladeren, P. J., and Rietjens, I. M. C. M. (2007). Tandem Mass Spectrometry Analysis of N^2-(*trans*-Isoestragol-3′-yl)-2′-deoxyguanosine as a strategy to study species differences in sulfotransferase conversion of the proximate carcinogen 1′-hydroxyestragole. *Chem. Res. Toxicol.* **20**, 991–998.

Punt, A., Freidig, A. P., Delatour, T., Scholz, G., Boersma, M. G., Schilter, B., Van Bladeren, P. J., and Rietjens, I. M. C. M. (2008). A physiologically based biokinetic (PBBK) model for estragole bioactivation and detoxification in rat. *Toxicol. Appl. Pharmacol.* **231**, 248–259.

Quick, D. J., and Shuler, M. L. (1999). Use of *in vitro* data for construction of a physiologically based pharmacokinetic model for naphthalene in rats and mice to probe species differences. *Biotechnol. Prog.* **15**, 540–555.

Randerath, K., Haglund, R. E., Phillips, D. H., and Reddy, M. V. (1984). ^{32}P-post-labelling analysis of DNA adducts formed in the livers of animals treated with safrole, estragole and other naturally-occurring alkenylbenzenes. I. Adult female CD-1 mice. *Carcinogenesis* **5**, 1613–1622.

Sangster, S. A., Caldwell, J., Hutt, A. J., Anthony, A., and Smith, R. L. (1987). The metabolic disposition of [methoxy-^{14}C]-labeled trans-anethole, estragole and *p*-propylanisole in human volunteers. *Xenobiotica* **17**, 1223–1232.

Scientific Committee on Food (SCF). (2001). Opinion of the scientific committee on food on estragole (1-allyl-4-methyxybenzene). Available at: http://ec.europa.eu/food/fs/sc/scf/out104_en.pdf. Accessed May 29, 2009.

Shimada, T., Yamazaki, H., Mimura, M., Wakamiya, N., Ueng, Y., Genguerich, F. P., and Inui, Y. (1996). Characterization of microsomal cytochrome P450 enzymes involved in the oxidation of xenobiotic chemicals in human fetal liver and adult lungs. *Drug Metab. Dispos.* **24**, 515–522.

Smith, R. L., Adams, T. B., Doull, J., Feron, V. J., Goodman, J. I., Marnett, L. J., Portoghese, P. S., Waddell, W. J., Wagner, B. M., Rogers, A. E., *et al.* (2002). Safety assessment of allylalkoxybenzene derivatives used as flavouring substances—Methyl eugenol and estragole. *Food Chem. Toxicol.* **40**, 851–870.

Solheim, E., and Scheline, R. R. (1973). Metabolism of alkenebenzene derivatives in the rat I. p-Methoxyallylbenzene (estragole) and p-methoxypropenylbenzene (anethole). *Xenobiotica* **3**, 493–510.

Wiester, M. J., Winsett, D. W., Richards, J. H., Doerfler, D. L., and Costa, D. L. (2002). Partitioning of benzene in blood: Influence of hemoglobin type in humans and animals. *Environ. Health Perspect.* **110**, 255–261.

Wiseman, R. W., Fennell, T. R., Miller, J. A., and Miller, E. C. (1985). Further characterization of the DNA adducts formed by electrophilic esters of the hepatocarcinogens 1′-hydroxysafrole and 1′-hydroxyestragole *in vitro* and in mouse liver *in vivo*, including new adducts at C-8 and N-7 of guanine residues. *Cancer Res.* **45**, 3096–3105.

Wiseman, R. W., Miller, E. C., Miller, J. A., and Liem, A. (1987). Structure-activity studies of the hepatocarcinogenicities of alkenylbenzene derivatives related to estragole and safrole on administration to preweanling male C57BL/6J x C3H/HeJ F$_1$mice. *Cancer Res.* **47**, 2275–2283.

Wislocki, P. G., Miller, E. C., Miller, J. A., McCoy, E. C., and Rosenkranz, H. S. (1977). Carcinogenic and mutagenic activities of safrole, 1′-hydroxysafrole, and some known or possible metabolites. *Cancer Res.* **37**, 1883–1891.

Zangouras, A., Caldwell, J., Hutt, A. J., and Smith, R. L. (1981). Dose dependent conversion of estragole in the rat and mouse to the carcinogenic metabolite, 1′-hydroxyestragole. *Biochem. Pharmacol.* **30**, 1383–1386.